RSC Advances

PAPER

View Article Online
View Journal | View Issue

Cite this: *RSC Adv.*, 2021, **11**, 10847

Titanium–silicon ferrierites and their delaminated forms modified with copper as effective catalysts for low-temperature NH_3-SCR

Aneta Świeś,[a] Andrzej Kowalczyk,[a] Marek Michalik,[b] Urbano Díaz,[c] Antonio E. Palomares[c] and Lucjan Chmielarz[*a]

Received 10th February 2021
Accepted 5th March 2021

DOI: 10.1039/d1ra01139a

rsc.li/rsc-advances

Titanium–silicon ferrierites with different Si/Ti ratios and their delaminated forms were modified with copper by ion-exchange. The obtained samples were characterized with respect to their chemical composition (ICP-OES), structure (XRD), texture (N_2 sorption), morphology (SEM), form and aggregation of titanium and copper species (UV-vis-DRS), reducibility of deposited copper species (H_2-TPR) and surface acidity (NH_3-TPD). The porous structure of the zeolitic samples strongly influenced the form and aggregation of deposited copper species. In the case of the three dimensional microporous structure of ferrierites (Ti-FER), copper was deposited mainly in the form of aggregated copper oxide species, in contrast to the open micro- and mesoporous structure of delaminated ferrierites (Ti-ITQ-6), where mainly copper in the form of monomeric cations was identified. It was shown that monomeric copper cations are more catalytically active in NO to NO_2 oxidation than aggregated copper oxide species and, therefore, for the low-temperature conversion of nitrogen oxides the fast SCR reaction pathway is more effective for delaminated ferrierites modified with copper (Cu-Ti-ITQ-6) than for microporous three dimensional ferrierite catalysts (Cu-Ti-FER).

Introduction

Nitrogen oxides, NO_x including NO and NO_2, contribute to acid rain, photochemical smog, ozone layer depletion and greenhouse effects, and are therefore seriously dangerous for Earth's ecosystems and human health. The main NO_x emitters are mobile sources, such as diesel vehicles, and stationary sources, such as power plants and industrial boilers.[1,2] The major technologies used for the control of nitrogen oxide emissions from stationary and mobile sources are based on catalytic NO_x reduction with ammonia.[3,4] Commercial NH_3-SCR catalysts used for stationary sources, based on V_2O_5–WO_3/TiO_2 and V_2O_5–MoO_3/TiO_2 oxide systems, effectively operate in the temperature range of 300–400 °C with a relatively high selectivity to nitrogen and resistance for SO_x poisoning.[5,6] The BlueTec technology, used for the NO_x emission control in diesel vehicles, is based on the on-board ammonia production by urea hydrolysis and, similarly to classical NH_3-SCR, using ammonia as reducing agent for the catalytic NO_x conversion.[7,8] The studies focused on the improvement of these technologies' efficiency are still continuing. One of the major current challenges in this area is development of the low-temperature NH_3-SCR technology that allows the NO_x to N_2 conversion at temperatures below 250 °C. Development of such a technology could result in the retrofitting of the currently used installations for the treatment of flue gases emitted from stationary sources (*e.g.*, electric power stations) and therefore increase their efficiency and decrease operation costs. In most of the contemporary installations the NH_3-SCR units are located upstream of electrostatic precipitator (ESP) and therefore, such unites operate with dusty gas stream (high-dust SCR), what may result in clogging of channels in the catalytic monoliths by dust particles. This problem could be solved by de-dusting of flue gases in ESP prior to the NH_3-SCR unit (low-dust SCR). Unfortunately, ESP operates with the relatively cold flue gases of temperature about 250 °C or even lower. Thus, such de-dusted gases, downstream of ESP unit, should be heated to above 300 °C prior to the NH_3-SCR converter.[9] Therefore, such solution needs additional operation costs of flue gases heating. Development of the effective NH_3-SCR catalyst operating at low temperatures could enable retrofitting of the installations of flue gases treatment resulting in increased efficiency of flue gases purification and reduction operation costs. The catalysts containing copper,[10] manganese[11] and iron[12] were reported to operate in the low-temperature range. The very promising results of low-temperature NH_3-SCR were obtained for zeolites

[a]*Jagiellonian University in Kraków, Faculty of Chemistry, Gronostajowa 2, 30-387 Kraków, Poland. E-mail: chmielar@chemia.uj.edu.pl; Tel: +48 126862417*

[b]*Jagiellonian University in Kraków, Institute of Geological Sciences, Gronostajowa 3a, 30-387 Kraków, Poland*

[c]*Instituto de Tecnología Química, Universitat Politècnica de València – Consejo Superior de Investigaciones Científicas, Avd. de los Naranjos s/n, 46022 Valencia, Spain*

modified with copper.[13,14] It was shown that a very important role in such low-temperature process is assigned to so called fast SCR reaction ($2NH_3 + NO + NO_2 \rightarrow 2N_2 + 3H_2O$). NO_2, which is needed for this reaction can be added to the gas stream[14] or generated *in situ* by partial oxidation of NO to NO_2 in flue gas stream.[12,15] The second option seems to be much more convenient, especially for the large-scale applications, however needs development of the catalysts simultaneously active in NO to NO_2 oxidation and in the NH_3-SCR reaction.

Our previous studies[15] have shown a very promising catalytic performance of delaminated ferrierites modified with copper in the low-temperature NH_3-SCR process, what was assigned to the activity of these catalysts in NO to NO_2 oxidation. The present studies are also focused on delaminated titanium–silicon ferrierites modified with copper as catalysts of the NH_3-SCR process. The concept of the aluminum for titanium replacement in the zeolite framework follows from the literature reports showing important role of titanium interacting with transition metal species in NO to NO_2 oxidation.[12,16–23] Thus, the main goal of the presented studies was verification of the catalytic performance of the microporous and delaminated titanium–silicon ferrierites as potential catalysts for the low-temperature NH_3-SCR process. Moreover, the catalytic performance of the catalysts based on Ti-zeolites and Al-zeolites was compared and discussed.

Experimental section

Synthesis of Ti-PREFER and Ti-FER

Zeolite precursor materials with titanium in the zeolite framework (Ti-PREFER) were synthesized by mixing of 4-amino-2,2,6,6-tetramethylpiperidine (R, Fluka, Germany) used as a structure directing agent, titanium(IV) ethoxide (98%, Alfa Aesar, Haverhill, MA, USA) as titanium source, silica Aerosil 200 (Evonik Industries AG, Essen, Germany) as silicon source, NH_4F (98%, Sigma-Aldrich, St. Louis, MO, USA), HF (49.8%, Sigma-Aldrich, St. Louis, MO, USA) and distilled water. For the synthesis of the zeolitic samples the following reactants with the suitable ratios were used: $1SiO_2 : xTiO_2 : 1R : 1.5NH_4F : 0.5HF : 10H_2O$, where $x = 0.04$, 0.02 and 0.01 was for the samples with the Si/Ti intended molar ratios of 25, 50 and 100, respectively. The resulting slurries were placed in autoclaves at 135 °C for 11 days. The solid product was filtrated, washed with distilled water, and dried overnight at 60 °C. The obtained zeolite precursors are denoted as Ti-PREFER-25, Ti-PREFER-50, and Ti-PREFER-100, respectively for the samples with the intended molar Si/Ti ratio of 25, 50, and 100. To produce three dimensional (3D) ferrierite zeolites, Ti-PREFER-25, Ti-PREFER-50 and Ti-PREFER-100 precursors were calcined at 600 °C for 6 hours resulting in the samples denoted as Ti-FER-25, Ti-FER-50 and Ti-FER-100.

Ti-ITQ-6 synthesis

To prepare the ITQ-6-type materials, 10 g of the lamellar precursor (Ti-PREFER) were dispersed in 40 g of H_2O MilliQ, and 200 g of a cetyltrimethylammonium hydroxide solution (29 wt%, 30% exchanged Br/OH) and 60 g of a solution of tetrapropylammonium hydroxide (40 wt%, 30% exchanged Br/OH), being the final pH ~ 12.5. The resultant mixture was heated at 80 °C, stirring vigorously, for 16 h to produce the swelling of the layers of the precursor material. At this point, this suspension was sonicated in an ultrasound bath (50 W, 40 kHz) for 1 hour to disperse the individual sheets. Then, the pH was decreased to 3.0 by adding HCl (6 M) to facilitate the flocculation of the expanded solids that were recovered by centrifugation, washed with distilled water, and dried at 60 °C for 12 h to obtain the ITQ-6-type materials. The solids were calcined for 3 hours at 540 °C in N_2 and then during 7 hours in air (fluxe 2.5 mL s^{-1}, heating rate 3 °C min^{-1}), resulting in the samples denoted as Ti-ITQ-6-25, Ti-ITQ-6-50, and Ti-ITQ-6-100, respectively for the zeolites with the intended Si/Ti molar ratios of 25, 50, and 100.

Copper deposition into zeolites

Copper was deposited into series of the Cu-Ti-FER and Cu-Ti-ITQ-6 samples by ion-exchange method using copper acetate as copper precursor. The zeolite sample was dispersed in 0.06 M aqueous solution of $Cu(CH_3COO)_2 \cdot H_2O$ (10 g of solid sample per 1000 g of solution) and the obtained slurry was stirred at 80 °C for 6 h. Then, the solid product was separated by filtration, washed with distilled water, dried overnight at 60 °C, and finally calcined at 550 °C for 8 h.

Catalysts characterization

The structure of the obtained samples was analysed by XRD method. The measurements were conducted in a Bruker D2 Phaser diffractometer (Bruker, Billerica, MA, USA), in 2θ range of 2–40° with a step of 0.02° and a counting time of 1 s per step.

The textural parameters of the samples were determined by low-temperature sorption of nitrogen at −196 °C using a 3Flex (Micrometrics, Norcross, GA, USA) automated gas adsorption system. Prior to the measurement each zeolite sample was outgassed under a vacuum at 350 °C for 24 h. The specific surface area of the samples was determined using the BET (Brunauer–Emmett–Teller) equation. Horvath–Kawazoe model was applied for determination of pore size distribution in the micropore range, while BJH (Barrett–Joyner–Halenda) model in the mesopore range. The total pore volume was determined based on the total amount of adsorbed nitrogen at relative pressure $p/p_0 = 0.98$. The chemical composition of the samples was analysed by inductively coupled plasma-optical emission spectrometry (ICP-OES) using iCAP 7400 instrument (Thermo Scientific, Waltham, MA, USA). The powder samples were dissolved in a mixture of mineral acids composed of hydrofluoric (high purity grade, Honeywell, Charlotte, NC, USA), hydrochloric (high purity grade, Honeywell, Charlotte, NC, USA) and nitric acid (high purity grade, Honeywell, Charlotte, NC, USA). Dissolution of the solid samples was conducted with the assistance of microwave radiation using Ethos Easy system (Milestone, Sorisole, Italy). The form and aggregation of titanium and copper species introduced into the zeolitic samples were analysed by UV-vis-DR spectroscopy using an Evolution

600 spectrophotometer (Thermo Scientific, Waltham, MA, USA) operating in the range of 200–900 nm with a resolution of 2 nm. SEM images of the samples were recorded using Hitachi S-4700 scanning electron microscope equipped with a Noran Vantage analyser. The reducibility of the copper species deposited into zeolite samples was analysed by temperature-programmed reduction with using H_2 as reducing agent (H_2-TPR). The measurements were carried out in a fixed-bed flow microreactor system equipped with thermal conductivity detector (Valco). The flow rate of gas mixture was adjusted and controlled by mass flow controllers (Brooks Instrument). Prior to the H_2-TPR runs, each sample (15 mg) was outgassed in a flow of pure argon at 600 °C for 30 min. After cooling to 100 °C the H_2-TPR runs were carried out in the range of 100 to 800 °C with the linear heating rate of 10 °C min^{-1} in a flow of gas mixture containing 5.0 vol% of H_2 diluted in argon (flow rate – 5 mL min^{-1}). Temperature-programmed desorption of ammonia (NH_3-TPD) was used for analysing of the surface acidity of the zeolitic samples. Prior to NH_3-TPD run, the sample of zeolite (50 mg), placed in fixed-bed quartz microreactor, was outgassed at 600 °C for 30 min. Then, microreactor with the sample was cooled to 70 °C and saturated in the flow of ammonia (1 vol% NH_3 diluted in helium, 20 mL min^{-1}) followed by flushing with pure helium to remove ammonia physiosorbed on the sample surface. Finally, the temperature-programmed desorption of ammonia (NH_3-TPD) was carried out with a linear heating rate of 10 °C min^{-1} in a flow of pure helium (20 mL min^{-1}). All experimental stages were monitored by a quadrupole mass spectrometer – QMS (PREVAC, Rogów, Poland) connected directly to the microreactor outlet *via* heated line.

Catalytic studies

NH_3-SCR. Copper modified Ti-zeolites were tested as catalysts of selective catalytic reduction of NO with ammonia (NH_3-SCR). The sample of catalyst (100 mg) was placed in fixed-bed quartz microreactor and pre-treated in a flow of pure helium (20 mL min^{-1}) at 550 °C for 30 min. Then, the microreactor with catalyst was cooled to 100 °C, and a flow of helium was exchanged for flow of gas mixture containing 0.25 vol% NO; 0.25 vol% NH_3; 2.5 vol% O_2 diluted in helium (total flow rate of 40 mL min^{-1}). Catalytic tests were done in the range of 100–350 °C with intervals of 25 °C. The concentrations of reactants were continuously monitored by a quadrupole mass spectrometer (QMS, PREVAC, Rogów, Poland) connected directly to the reactor outlet. Moreover, for the selected catalyst the stability isothermal test with the periodical changes from dry (composition this same as in polythermal tests) to wet (0.25 vol% NO; 0.25 vol% NH_3; 2.5 vol% O_2 and 3.5 vol% H_2O diluted in helium) reaction mixture was done. Water vapor was introduced into reaction mixture by using of saturator containing distilled water. Helium was flowing through the saturator, which was kept in isothermal conditions (0 °C, thermostat). Gas lines were heated by heating tapes to avoid water vapor condensation.

AMOx. In the case of ammonia oxidation (AMOx) studies, similarly to NH_3-SCR, the sample of 100 mg was placed in fixed-bed quartz microreactor and outgassed at 550 °C for 30 min in a flow of pure helium (20 mL min^{-1}). Catalytic tests were conducted in the range of 100–350 °C, with intervals of 50 °C, in a flow of gas mixture containing 0.5 vol% NH_3 and 2.5 vol% O_2 diluted in helium (total flow rate of 40 mL min^{-1}). Concentrations of reactants were continuously monitored by a quadrupole mass spectrometer (QMS, PREVAC, Rogów, Poland) connected directly to the reactor outlet *via* heated line.

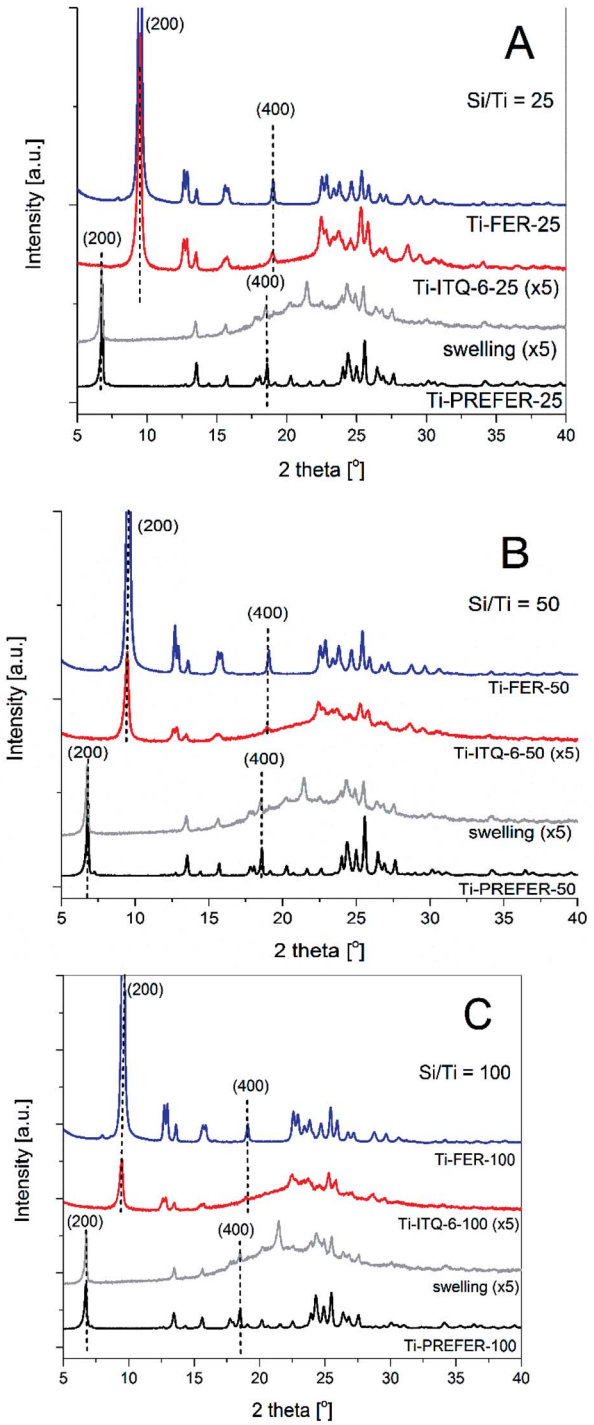

Fig. 1 X-ray diffractograms of titanium–silicon ferrierite based samples (Ti-PREFER, swollen Ti-PREFER, delaminated Ti-ITQ-6 and Ti-FER) with the intended molar Si/Ti ratios of 25 (A), 50 (B) and 100 (C).

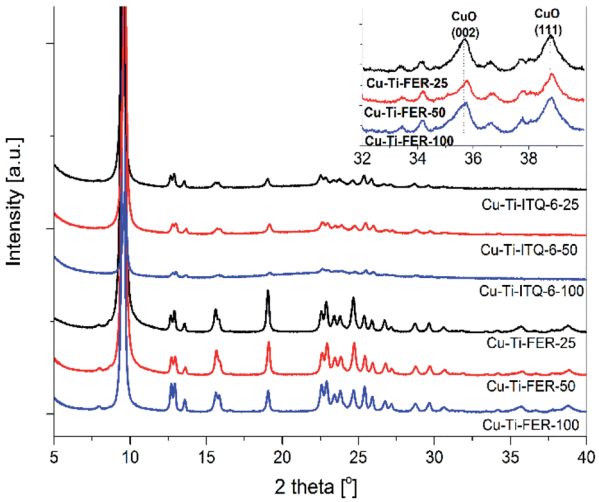

Fig. 2 X-ray diffractograms of titanium–silicon ferrierites (Cu-Ti-FER series) and their delaminated forms modified with copper (Cu-Ti-ITQ-6 series).

NO to NO_2 oxidation. The reaction of NO to NO_2 oxidation was carried out in the same system as in the case of NH_3-SCR and AMOx processes. The only difference was replacement of QMS for FTIR spectrometer. The reaction was studied in a flow of gas mixture containing 0.5 vol% NO and 2.5 vol% O_2 diluted in helium (total flow rate of 40 mL min^{-1}). FTIR spectrometer Nicolet iS5 (Thermo Scientific, Waltham, MA, USA) equipped with a gas cell of 10 cm length, operating in the wavenumber range of 625–4000 cm^{-1} with a resolution of 4 cm^{-1}, was used for the analysis of reaction mixture down-stream and up-stream of microreactor. The NO_2 and NO concentrations in the reaction mixture were determined by the analysis of the bands at 1593 and 1912 cm^{-1}, respectively.

Results and discussion

The structure of the zeolitic samples and their precursors were verified by X-ray diffraction method (Fig. 1). In diffractograms of the zeolite precursors – Ti-PREFER-25, Ti-PREFER-50, and Ti-PREFER-100 – the (200) diffraction peak at 2θ about 6.8°, indicating the interlayer distance of 1.3 nm, was identified.[24] The layered structure of the zeolite precursors is also proved by the presence of the (400) diffraction peak located at 2θ about 18.5°. Other peaks in diffractogram of the zeolite precursors are typical of the ferrierite structure,[24] that proves, independently of the intended Si/Ti molar ratio, the successful synthesis of the zeolite precursors. Calcination of the zeolite precursors resulted in a shift of the (200) and (400) diffraction peaks into higher values of 2θ angle characteristic of the sticked together zeolite layers and therefore indicating the condensation of such layers under calcination conditions with the formation of three dimensional (3D) ferrierite structure. Depending on the intended Si/Ti molar ratio – 25, 50, and 100 – the obtained ferrierite samples are denoted as Ti-FER-25, Ti-FER-50, and Ti-FER-100, respectively.

Preparation of Ti-ITQ-6 zeolite requires swelling and delamination of the zeolite precursors. Swelling of the zeolite precursors in strongly basic conditions resulted in a very significant intensity decrease of the (200) and (400) diffraction peaks (Fig. 1), indicating the formation of delaminated structure of the zeolite layers (the structure of "house of card" with non-parallel orientation of layers). The residual (200) and (400) diffraction peaks in diffractograms of the swollen precursors indicate that small fraction of the zeolite layers was not successfully swollen. Comparison of the intensities of these reflections cannot demonstrate any correlation between the Si/Ti molar ratio in the zeolite precursors and their susceptibility to be swelled. The swelling process, conducted under strongly basic conditions, resulted in a partial leaching of silicon from the zeolite layers. Possibly amorphous silica aggregates were formed in solution and deposited on the external surface of the zeolite grains. The broad diffraction peaks at about 15–30°, present in diffractograms of all swollen precursors, are characteristic of amorphous silica.[25]

In the next step, the swollen zeolite precursors were sonicated, followed by their calcination, resulting in a series of Ti-ITQ-6 zeolites with different intended Si/Ti molar ratios. In diffractograms of these samples, the low-intensive (200) reflections at 2θ about 9.6°, characteristic of the ferrierite structure,

Table 1 Textural parameters, acidity, molar Si/Ti ratios and copper content of Ti-FER, Ti-UTQ-6 zeolites and its copper modified forms

Sample	S_{BET} [m^2 g^{-1}]	V_{micro} [cm^3 g^{-1}]	V_{meso} [cm^3 g^{-1}]	C_a [μmol g^{-1}]	D_a [μmol m^{-2}]	Si/Ti [mol mol^{-1}]	Cu [wt%]
Ti-FER-25	364	0.129	0.115	59	0.16	37	—
Ti-FER-50	368	0.138	0.087	50	0.14	60	—
Ti-FER-100	367	0.135	0.102	45	0.12	132	—
Ti-ITQ-6-25	538	0.033	0.913	102	0.19	33	—
Ti-ITQ-6-50	615	0.016	1.376	70	0.11	78	—
Ti-ITQ-6-100	598	0.010	1.165	30	0.05	113	—
Cu-Ti-FER-25	324	0.119	0.100	48	0.15	30	4.8
Cu-Ti-FER-50	330	0.122	0.088	54	0.16	69	2.7
Cu-Ti-FER-100	317	0.119	0.091	83	0.26	124	4.8
Cu-Ti-ITQ-6-25	501	0.031	0.752	157	0.31	32	2.9
Cu-Ti-ITQ-6-50	523	0.031	0.782	142	0.27	76	2.8
Cu-Ti-ITQ-6-100	551	0.030	0.969	141	0.26	109	2.4

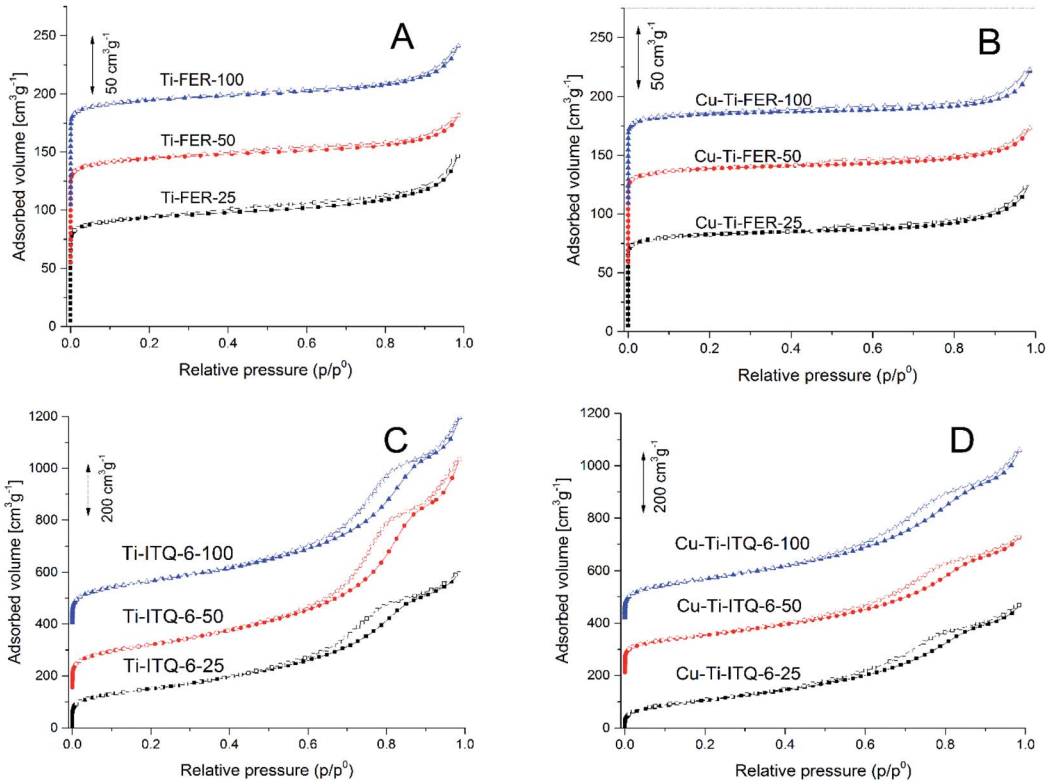

Fig. 3 Nitrogen adsorption desorption isotherms of the Ti-FER (A) and Ti-ITQ-6 (C) samples and their modifications with copper – Cu-Ti-FER (B) and Cu-Ti-ITQ-6 (D).

are present (Fig. 1). Intensities of these reflections are very low in comparison to a series of 3D ferrierite zeolites, indicating that only small fraction of the zeolite layers was not effectively separated by swelling process and condensed during calcination process. Depending on the intended Si/Ti molar ratio – 25, 50, and 100 – the obtained samples are denoted as Ti-ITQ-6-25, Ti-ITQ-6-50, and Ti-ITQ-6-100, respectively. It should be noted that the intensity of the (200) diffraction peak in a series of the Ti-ITQ-6 samples increases with a decrease in the intended Si/Ti molar ratios (Fig. 1), indicating that titanium incorporated into the zeolite layers favours their condensation.

Introduction of copper into zeolites by ion-exchange method did not result in any significant changes in diffractograms, indicating that the zeolite structures were not damaged by metal deposition (Fig. 2). However, in diffractograms of the Ti-FER samples the broad and low-intensive reflections, characteristic of CuO crystallites were identified (Fig. 2, insert). Such diffraction peaks were not found in diffractograms of the Ti-ITQ-6 samples. Thus, at least part of copper introduced into the Ti-FER samples formed crystallites of CuO.

The real values of the molar Si/Ti ratios, determined by chemical analysis and presented in Table 1, are higher that the intendent values. It shows that silicon was preferentially incorporated into the ferrierite layers comparing to titanium. The copper loading in the series of the Ti-FER samples is in the range of 2.7 to 4.8 wt% (Table 1). The correlation between the Si/

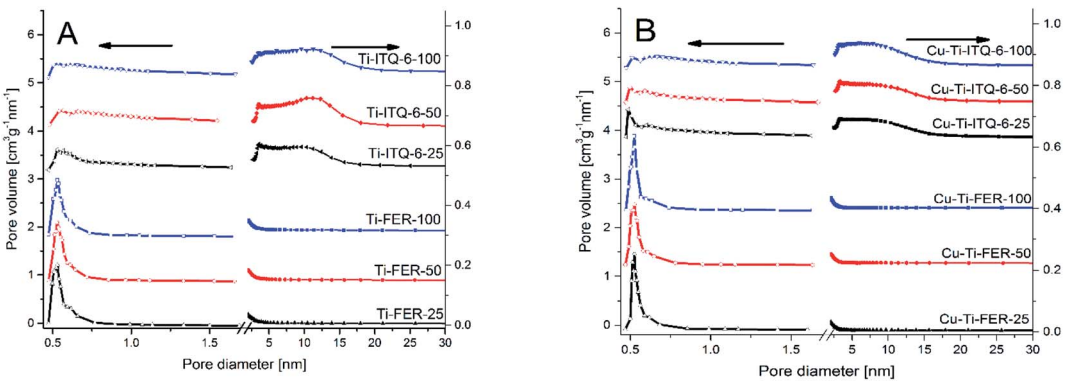

Fig. 4 Pore size distributions determined for Ti-FER and Ti-ITQ-6 (A) as well as their copper modified forms (B).

Ti molar ratio and copper content in the samples of this series was not found. In the case of the Ti-ITQ-6 series the copper loading is in the range of 2.4–2.9 wt% and decreases with a decrease in the Si/Ti molar ratio.

The nitrogen adsorption–desorption isotherms recorded for the zeolitic samples are presented in Fig. 3, while their textural parameters are compared in Table 1. The isotherms determined for the Ti-FER samples (Fig. 3A) are classified as type I according to the IUPAC definition[26] and are characteristic of microporous materials. The characteristic feature of these isotherms is an adsorption step at very low relative pressure indicating capillary condensation of nitrogen inside micropores. Deposition of copper into the Ti-FER samples did not resulted in modification of their microporous character (Fig. 3B). The isotherms of the Ti-ITQ-6 samples belong to type IV according to the IUPAC standards[26] and are characteristic of mesoporous materials (Fig. 3C). An adsorption step in the low range of the relative pressure indicates the presence of micropores, while an increase in nitrogen adsorbed volume in the p/p_0 range of 0.5–0.9 is characteristic for mesopores with a relatively broad pore size distribution. Thus, the isotherms recorded for the Ti-ITQ-6 samples indicate bimodal type of porosity. Channels in the zeolite layers are micropores, while the spaces between non-parallel oriented (delaminated) zeolite layers are mesopores. The hysteresis loops present in isotherms of Ti-ITQ-6 zeolites belong to H3 category, characteristic of non-rigid aggregates of plate-like particles.[26] The neckings in the hysteresis loops could be a result of partial plugging of mesopores.[27] Copper deposited into the Ti-ITQ-6 samples did not result in significant changes in isotherm profiles, thus bimodal micro- and mesoporous character was also present in the Cu-Ti-ITQ-6 samples (Fig. 3D). BET specific surface area (S_{BET}) of all the samples of the Ti-FER series is very similar and is in the range of 364–368 $m^2\ g^{-1}$ (Table 1). Deposition of copper into the Ti-FER samples resulted in a decrease of S_{BET} by about 10–14%. The samples of the Ti-ITQ-6 series are characterized by S_{BET} in the range of 538–615 $m^2\ g^{-1}$ as well as micropore volume (V_{micro}) significantly reduced and mesopore volume (V_{meso}) significantly increased in comparison to the Ti-FER samples (Table 1). Deposition of copper into the Ti-ITQ-6 samples reduced their S_{BET} by about 6 to 15%.

In the profiles of pore size distributions (PDS) determined for the Ti-FER samples, presented in Fig. 4A, the main maximum is located at about 0.50–0.53 nm and is characteristic of 10 MR (10-member ring) sub-units present in ferrierites.[28] Any peaks in the PSD profiles of the Ti-FER samples were found in the mesoporous range proving the microporous character of these samples. Introduction of copper into these zeolites did not result in any significant changes in the PSD profiles (Fig. 4B). In the case of the Ti-ITQ-6 samples the maximum PSD, characteristic of 10 MR diameter, is significantly reduced (Fig. 4A), that is associated to the microporous structure limited only to the zeolite layers in contrast to the microporous three-dimensional structure of the Ti-FER samples. The tail from the side of larger micropores, present in the PSD profiles of Ti-ITQ-6, indicates significant heterogeneity in micropore size distribution possibly caused by partial destruction of the zeolite layers under swelling and delamination conditions. The PSD profiles of the Ti-ITQ-6 samples are characterized by broad maxima in the mesopore range, typical of delaminated layered structure (Fig. 4A). The PSD profiles consist of sharp peak at about 3.5 nm and broad maximum centred at about 10–12 nm. As it was shown by XRD studies (Fig. 1), in the ITQ-6 samples the presence of amorphous silica formed under swelling conditions was proved and therefore mesopores present in such silica may contribute to the overall porosity of these materials. Introduction of copper into Ti-ITQ-6 decreased intensity of the broad maximum in the PSD profiles, indicating preferential location of copper species in mesopores (Fig. 4B). On the other side, the position of the maximum characteristic of 10 MR channels was slightly shifted from 0.50–0.53 nm to about 0.48–0.50 nm after copper introduction, indicating deposition of this metal also inside micropores.

The form and aggregation of titanium and copper in the zeolitic samples were studied by using UV-vis DR spectroscopy (Fig. 5). The spectra recorded for the series of the Ti-FER and Ti-ITQ-6 samples, presented in Fig. 5A, contain an intensive band at about 220 nm, characteristic of monomeric tetrahedrally coordinated titanium cations in the zeolite framework.[29,30]

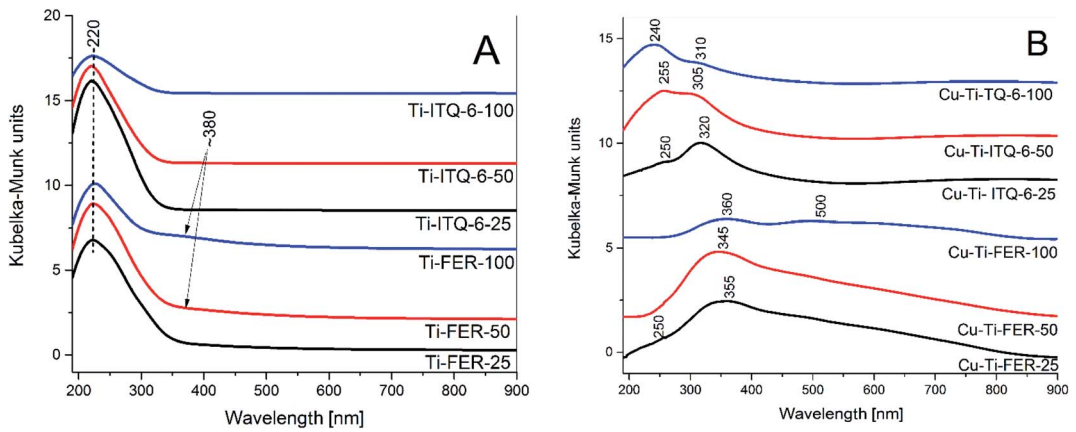

Fig. 5 UV-vis DR spectra of Ti-FER and Ti-ITQ-6 zeolites (A) and their copper modified forms – differential spectra (B).

Thus, in the Ti-ITQ-6 samples only titanium incorporated into zeolite framework was identified. In a series of Ti-FER zeolites, apart from the main band at 220 nm, broad and low-intense shoulder from the side of higher wavelengths was found. This latter band is associated to titanium in the form of extraframework species of various aggregations, from small polymerized hexacoordinated Ti-species containing Ti–O–Ti bridges to small aggregates of TiO_2.[29,30] It seems possible that such extraframework titanium species were extracted to solution from the zeolite precursors during swelling and delamination processes.

The differential spectra, obtained by subtracting of the original spectrum of the zeolitic support from the spectrum of its copper modified form, were used for the analysis of type and aggregation of deposited copper species (Fig. 5B). In the spectra of the Ti-FER samples dominate the band located at about 350–360 nm, characteristic of small oligomeric copper oxide species.[17,18] Only in the Cu-Ti-FER-25 sample, the shoulder at about 250 nm, indicating the presence of monomeric copper cations, was found. Such shoulder was not identified in the spectra of Cu-Ti-FER-50 and Cu-Ti-FER-100. The broad band centred at about 500 nm in the spectrum of Cu-Ti-FER-100 indicates a significant contribution of CuO crystallites in this sample.[17,18] The presence of such crystallites in Cu-Ti-FER-50 and Cu-Ti-FER-25 indicates shoulder above 400 nm. Thus, copper in the form or oligomeric copper species and copper oxide crystallites dominates in the series of the Cu-Ti-FER samples. Only in the case of Cu-Ti-FER-25 the contribution of monomeric copper cations was proved by the presence of shoulder at about 240–250 nm.[17,18] In the spectra of the Cu-Ti-ITQ-6 samples, the bands at about 240–250 and 305–330 nm dominate (Fig. 5B). The first band is assigned to monomeric copper ions interacting with oxygen of the zeolite framework ($O^{2-} \rightarrow Cu^{2+}$).[15] The presence of such monomeric copper cations in these samples is also proved by the broad bands above 550 nm, indicating d–d transition phenomena occurred in surface Cu^{2+} cations in pseudo-octahedral coordination interacting with water molecules.[31,32] The band at about 305–330 nm is assigned to the presence of oligomeric copper species, while the small shoulder above 400 nm is possibly related to small contribution of copper oxide crystallites.[17,18] It should be noted that intensity of the band characteristic of monomeric copper cations (about 250 nm) is significantly less intense for the Cu-Ti-ITQ-6-25 sample than for Cu-Ti-ITQ-6-50 and Cu-Ti-ITQ-6-100 indicating that there is a lower contribution of such dispersed copper species in the former sample in comparison to later ones. In general, the results of the UV-vis DRS analysis of the samples are in full agreement with XRD studies, which proved the presence of CuO crystallites only in the series of Cu-Ti-FER samples.

SEM micrographs of the zeolite samples modified with copper are presented in Fig. 6. In the case of the Cu-Ti-FER samples large two-dimensional crystallites of zeolite can be seen. The size of these crystallites decreases with an increase in the Si/Ti ratio. This observation agrees with the results of XRD analysis (Fig. 2), were intensity of the characteristic reflections increased with an increase in the Si/Ti ratio. Moreover, for the Cu-Ti-FER-50 and Cu-Ti-FER-100 samples small aggregates of amorphous silica are deposited on the surface of the zeolite

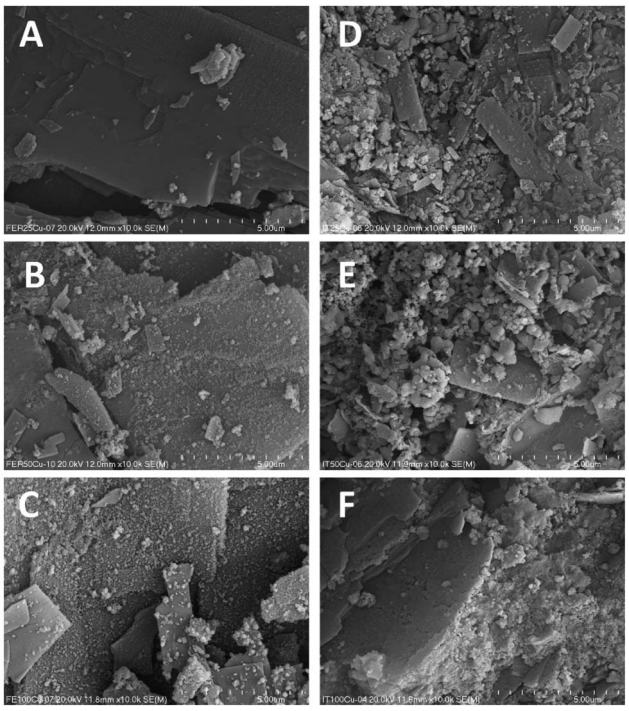

Fig. 6 SEM micrographs of Ti-FER and Ti-ITQ-6 with intended molar Si/Ti ratios of 25 (A, D), 50 (B, E), 100 (C, F), respectively.

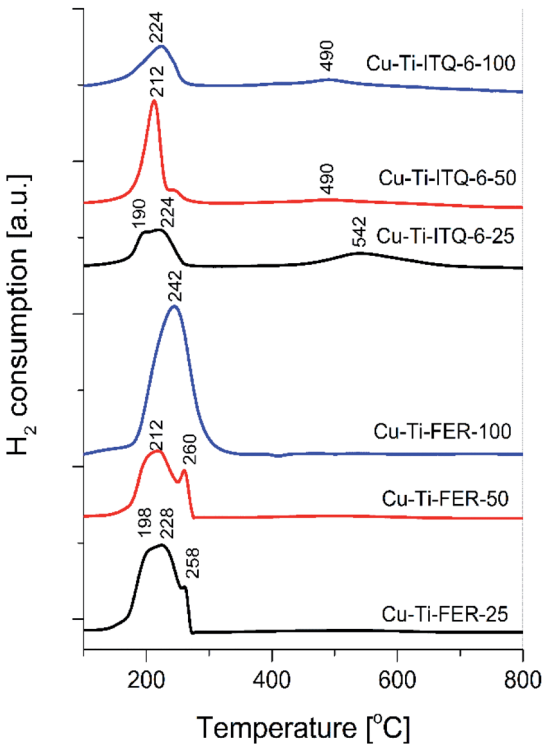

Fig. 7 H_2-TPR profiles of Ti-FER and Ti-ITQ-6 samples modified with Cu.

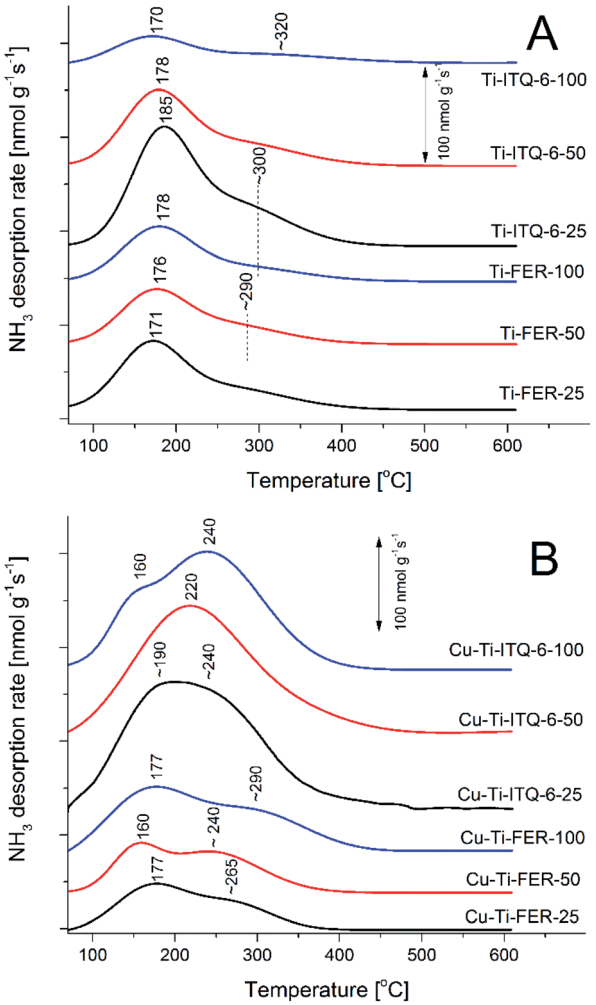

Fig. 8 NH_3-TPD profiles of obtained for Ti-FER and Ti-ITQ-6 zeolites (A) and their copper modified forms (B).

crystals. The EDS analysis of such aggregates showed that apart from silicon they contain also small amount of titanium and copper. The Cu-Ti-ITQ-6 samples are characterised by the presence of smaller two-dimensional crystallites of zeolite and moreover significant contribution of small amorphous silica aggregates containing small amounts of copper and titanium. Such amorphous silica was detected for this series of the samples by the XRD analyses (Fig. 1).

The H_2-TPR profiles of the zeolitic samples modified with copper, shown in Fig. 7, are characterized by two temperature ranges of copper species reduction. The low-temperature region at temperatures below 300 °C is characteristic of the reduction of Cu^{2+} to Cu^0 in aggregated copper oxide species as well as reduction of monomeric Cu^{2+} cations and small oligomeric copper species to Cu^+.[16] The second step of such dispersed copper species reduction, Cu^+ to Cu^0, takes place at temperatures above 300 °C.[16] In the case of the samples of Cu-Ti-FER series the low-temperature peaks dominate indicating mainly the presence of the aggregated copper oxide species. The splitting of the low-temperature peaks, observed in reduction profiles of Cu-Ti-FER-25 and Cu-Ti-FER-50, is possibly attributed to the presence of copper oxide species of different aggregation. For the samples of the Cu-Ti-ITQ-6 series, apart from the low-temperature reduction peaks, also high-temperature peaks are present, indicating significant contribution of the highly dispersed copper species. Thus, the obtained results are in full agreement with the results of XRD (Fig. 1) and UV-vis DRS (Fig. 5) studies.

Temperature-programmed desorption of ammonia (NH_3-TPD) method was used for evaluation of the surface concentration and relative strength of acid sites in the samples. On the other site, assuming that the majority of the proposed mechanisms of the NH_3-SCR process included chemisorption and activation of ammonia molecules as important reaction step,[5] the NH_3-TPD studies may also give some insight into the reaction mechanism. Ammonia desorption profiles of the Ti-FER and Ti-ITQ-6 samples, presented in Fig. 8A, are characterized by intensive maximum centred at about 170–185 °C and shoulder from the side of higher temperatures. Desorption of ammonia at relatively low temperatures indicates mainly the presence of sites of low acidic strength, possibly related to titanium incorporated into the zeolite framework. The role of such weak sites possibly come from ≡Ti–OH groups and Ti^{3+} cations generated *e.g.* charge relocation $(O^{2-}Ti^{4+}) \rightarrow (O^{-}Ti^{3+})$.[33]

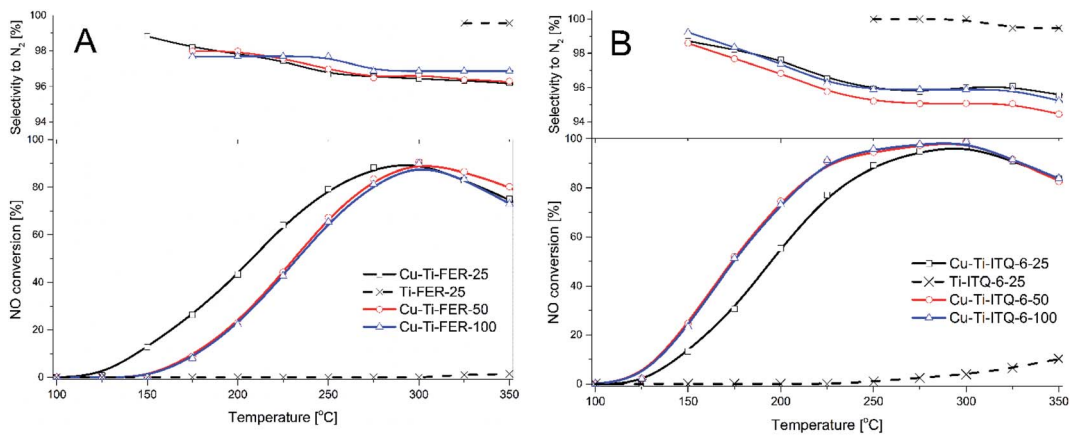

Fig. 9 Results of NH_3-SCR catalytic tests for copper modified Ti-FER (A) and Ti-ITQ-6 (B) catalysts.

Deposition of copper significantly changed ammonia desorption profiles (Fig. 8B) mainly by appearance of new maxima or shoulder centred at about 240–290 °C. Thus, it seems that these maxima are assigned to the interaction of copper with ammonia molecules, which is stronger in comparison to ammonia bounded to titanium species (*cf.* Fig. 8A). The possible interaction of ammonia molecules with copper cations is based on the accommodation of free electron pair of ammonia into unoccupied d-orbital of copper ($NH_3 \rightarrow Cu^{n+}$). The surface concentration (C_a) and surface density (D_a) of acid sites after copper deposition into the Ti-FER samples significantly changed (Table 1), decreasing for Cu-Ti-FER-25 and increasing for Cu-Ti-FER-50 and Cu-Ti-FER-100. Deposition of copper into the samples of the Ti-ITQ-6 series resulted in a significant increase of surface concentration of acid sites. Such difference is possibly related to accessibility of copper cations for ammonia molecules, that is much better in the case of the Cu-Ti-ITQ-6 samples containing highly dispersed copper species than in the case of the Cu-Ti-FER samples containing aggregated copper oxide species and crystallites.

Copper modified Ti-FER and Ti-ITQ-6 zeolites were studied as catalysts of the selective catalytic reduction of NO with ammonia (Fig. 9). In the series of Cu-Ti-FER catalysts the best results were obtained for the Cu-Ti-FER-25 sample (Fig. 9A). In this case the NO conversion started at about 100 °C and intensively increased to 300 °C reaching the level of 90%. At higher temperatures efficiency of the NO conversion decreased due to the side process of direct ammonia oxidation by oxygen present in the reaction mixture. The other two catalysts of this series, Cu-Ti-FER-50 and Cu-Ti-FER-100, presented significantly lower catalytic activity, especially in the low-temperature range. For these catalysts, the NO conversion started at about 125 °C and increased to nearly 90% at about 300 °C. The selectivity to nitrogen is above 95% for all the catalysts of this series in the studied temperature range (Fig. 9A). The difference in the catalytic performance between Cu-Ti-FER-25 and other catalysts of this series is possibly related to the higher contribution of copper in the form of monomeric cations, that was shown by UV-vis DRS studies (Fig. 5B). Thus, increased activity of Cu-Ti-FER-25 in comparison to other catalysts of this series could be related to higher activity of such dispersed copper species in NO reduction with ammonia in comparison to aggregated copper oxide species. Another important parameter of the samples that could influence their catalytic activity is copper loading. In the case of Cu-Ti-FER-25 and Cu-Ti-FER-100 here is the same copper content, but the former catalyst is significantly more active. Thus, the form of deposited copper species seems to be more important than the loading of this metal. This hypothesis is supported by the results of catalytic tests of the Cu-Ti-ITQ-6 samples (Fig. 9B), which contain lower copper loadings than Cu-Ti-FER-25 and Cu-Ti-FER-100 but are significantly more catalytically active in the NH_3-SCR process. Moreover, there is a significant contribution of copper in the form of monomeric copper cations, which was postulated to be more catalytically active than aggregated copper oxide species, in these catalysts (Fig. 5B). It should be noted that the lower activity of Cu-Ti-ITQ-6-25 than other catalysts of this series is possibly related to the lower contribution of monomeric copper cations in this sample comparing to Cu-Ti-ITQ-6-50 and Cu-Ti-ITQ-6-100 (Fig. 5B). The NO conversion above 90% was obtained in the range of 225–325 °C for the most active catalysts of this series (Fig. 9B). The selectivity to nitrogen was above 94% in the studied temperature range. The efficiency of the NO conversion decreased above 300 °C due to the side reaction of direct ammonia oxidation. The role of acid sites in the NH_3-SCR process is another important issue that should be considered. Comparison of acid site concentrations (C_a) and density (D_a) presented in Table 1 with the results of the catalytic NH_3-SCR tests (Fig. 9) shows that there is not clear correlation between these properties of the studied catalysts. As it was already mentioned the acid sites in the catalysts are assigned to the presence of titanium and copper. Thus, as it was shown by NH_3-TPR results, ammonia chemisorption occurs on both copper and titania acid sites. The zeolite samples non-modified with copper presented only very poor catalytic activity in the NH_3-SCR process (Fig. 9). Thus, titanium incorporated into the zeolite framework is inactive or only slightly active in proper activation of ammonia molecules into NH_3-SCR. Deposition of copper resulted in activation of the samples for the NO reduction with ammonia, thus copper species play a key role in activation of ammonia molecules for the NH_3-SCR process. As it was already stated, the form of deposited copper species strongly influences the activity of the catalysts, that proves the hypothesis of crucial role of copper in the NO conversion. Thus, it seems that ammonia molecules chemisorbed on the titanium acid sites do not directly take part in the NH_3-SCR process. On the other side, our previous studies of the NH_3-SCR process over aluminium–silicon Al-ITQ-6 modified with copper (intended Si/Al molar ratio of 50, Cu loading of 2.7 wt%, mainly in the form of monomeric copper cations) showed its catalytic activity at higher temperatures.[15] The NO conversion above 90% in the presence of Cu-Al-ITQ-6 was obtained in the range of 250–350 °C, thus at temperatures higher by about 25 °C in comparison to the Cu-Ti-ITQ-6-50 and Cu-Ti-ITQ-6-100 (Fig. 9B) catalysts. For both, Cu-Al-ITQ-6 and the Cu-Ti-ITQ-6 series of the samples, the catalytic tests were done under these same conditions. Thus, titanium incorporated into the zeolite framework possibly promotes conversion of NO with ammonia at temperatures lower comparing to silica–alumina zeolites.

Ammonia is bounded to titanium acid sites in the Ti-FER and Ti-ITQ-6 samples much weaker (Fig. 8A) comparing to Al-FER and Al-ITQ-6 zeolites[15] and therefore desorption of ammonia molecules takes place at lower temperatures. Ammonia molecules chemisorbed on titanium acid sites could be an ammonia reservoir deposited on the catalyst surface. Desorption of ammonia from such acid sites, which occurs for Ti-sites at temperatures lower than for Al-sites,[15] may supply additional portion of the reducing agent for the NO conversion. It should be noted that the main maximum of ammonia desorption for the Ti-FER and Ti-ITQ-6 samples is located at about 170–185 °C (Fig. 8A), while after copper deposition was shifted to about 190–240 °C for a series of the Cu-Ti-ITQ-6 samples (Fig. 8B). As it was reported in our previous studies for pure silica in the form of spherical MCM-41 modified with

Table 2 Comparison of the results of NH_3-SCR tests in the presence of various zeolites modified with copper

Catalyst	NO conversion at 250 °C [%]	Cu content [wt%]	GHSV [h^{-1}]	Reference
Cu-Ti-FER-25	78	4.8	24 000	This work
Cu-Ti-ITQ-6-100	95	2.4	24 000	This work
Cu-ZSM-5[a]	85	4.9	90 000	19
Cu-BETA[b]	73	5.8	90 000	19
Cu/SAPO-34[c]	96	1.5	40 000	20

[a] ZSM-5, Si/Al = 50, copper deposited by ion-exchange method. [b] BETA, Si/Al = 25, copper deposited by ion-exchange method. [c] SAPO-34, (Al + P)/Si = 7.35, copper deposited by impregnation method.

copper by template ion-exchange method the maximum of ammonia desorption maximum was located at about 240–260 °C and was assigned to the interaction with copper species.[18] Thus, it seems that in the case of the Cu-Ti-FER series a new peak with the maximum at about 240–290 °C, could be assigned to ammonia desorption from copper sites (Fig. 8B). Thus, the re-adsorption of ammonia molecules desorbing from weaker Ti-acid sites on stronger Cu-sites cannot be excluded. In general, desorption of ammonia from the acid Al-sites in Cu-Al-FER, Cu-Al-ITQ-6 occurred at temperatures higher by about 20–35 °C for the samples with higher aluminium content and moreover significant part of ammonia desorbed above 300 °C.[15] For the samples with lower aluminium content low temperature maximum of ammonia desorption is located at temperatures similar to that of the Ti-FER and Ti-ITQ-6 samples but significant amount of ammonia is desorbing above 300 °C.[15] Thus, the differences in the low-temperature activity of Ti- and Al-zeolites in NH_3-SCR are possibly related to different acid strength of titanium and aluminium sites and therefore deferent range of ammonia molecules desorption and possible re-adsorption and activation on the Cu-sites.

Another question is related to the role of porous structure of the zeolite samples in the NH_3-SCR process. It was observed that in the case of the microporous Ti-FER samples copper was deposited mainly in the form of aggregated copper oxide species. Copper cations present in an aqueous solution, used in ion-exchange procedure, exist in the form of octahedral aqua copper(II) complex, $[Cu(H_2O)_6]^{2+}$, with the size of about 0.57–0.66 nm. Such complexes are too large to be accommodated into the ferrierite channels (diameter of about 0.52 nm) and therefore are deported mainly on the outer surface of the zeolite grains. Calcination of such samples possibly resulted in the sintering of copper species loosely bounded to the zeolite surface with the formation of aggregated copper oxide species. On the other hand, interlayer spaces in the Ti-ITQ-6 samples are large enough to accommodate octahedral aqua copper(II) complexes. Possibly the main driving forces of copper species deposition are coulombic interactions of octahedral aqua copper(II) complexes and framework Ti^{3+} cations formed *e.g.* by charge relocation $(O^{2-}Ti^{4+}) \rightarrow (O^{-}Ti^{3+})$.[33] However, the comparison of copper loadings in the Cu-Ti-ITQ-6 samples and the Si/Ti molar ratios in these zeolites (Table 1) shows that apart from coulombic interactions also other mechanisms of copper species deposition cannot be excluded.

The NO conversion achieved at temperature of 250 °C over various zeolitic catalysts active in the process of NH_3-SCR are compared in Table 2. As it can be seen the most active catalyst from our studies, Cu-Ti-ITQ-6, belongs to the most effective low-temperatures catalysts reported in literature.[19,20] Of course, this is only rough comparison because of significantly different catalytic test conditions, such as various gas hour space velocity (GHSV) and composition of reaction mixture, as well as different copper loadings and its deposited forms. However, it seems that high dispersion of copper species deposited into the zeolite with open porous structure is a very beneficial for its high activity in the low-temperature NH_3-SCR process.

For the most active catalyst, Cu-Ti-ITQ-6-100, additional isothermal stability test with the periodical exchange from dry (gas mixture of the same composition as in polythermal tests) to wet (reaction mixture with addition of 3.5 vol% of water vapour) reaction mixture was done (Fig. 10). For the first 1 h of the test in a flow of dry reaction mixture at 250 °C, the NO conversion and selectivity to N_2 was on the stable level of about 93–94% and 96.5%, respectively. Exchange from dry to wet reaction mixture after first hour of the test resulted in a drop in the NO conversion to 92% and during next hour to 86.5%. Exchange for wet to

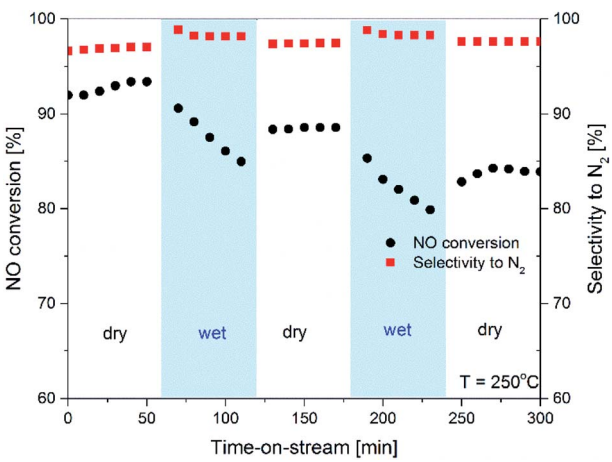

Fig. 10 Results of NH_3-SCR isothermal (250 °C) stability test for Cu-Ti-ITQ-6-100 catalysts.

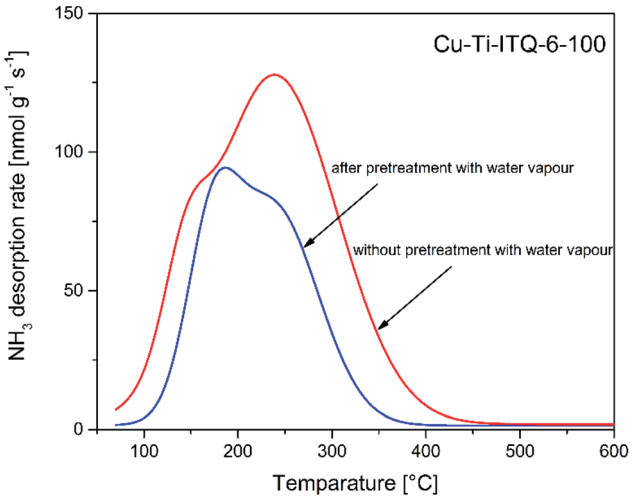

Fig. 11 Results of NH_3-TPD profiles obtained for the Cu-Ti-ITQ-6-100 sample with and without pre-treatment with water vapour prior to the ammonia adsorption.

dry reaction mixture caused an increase of the NO conversion to the level about 90%. Similar effects were observed during the subsequent changes from dry to wet and then from wet to dry reaction mixture. The final level of the NO conversion was about 85.5%, so decreased by about 8% in comparison to the initial conversion level. The selectivity to nitrogen increased by about 1.5–2.0% in a flow of wet reaction mixture. Probably, the main reason of the decreased NO conversion observed in the flow of wet reaction mixture is competitive adsorption of ammonia and water molecules on these same surface sites, possibly copper cations. To verify this hypothesis additional NH_3-TPD studies for the sample pre-treated with water vapour were done. In this case, the Cu-Ti-ITQ-6-100 catalyst was saturated in a flow of water vapor (3.5 vol%) in helium (20 mL min^{-1}) for 30 min and then NH_3-TPD run was done (under this same conditions as in earlier presented studies). As it was shown in Fig. 11 the ammonia desorption profile obtained for the sample pre-treated with water vapour is significantly less intensive comparing to the profile of this same catalyst but without pre-treatment with water vapour. Thus, under condition of the catalytic tests with the wet reaction mixture part of acid sites, which are possibly also active sites of NH_3-SCR, is blocked by adsorbed water molecules. Of course, it resulted in the decreased NO conversion, what was observed in our studies (Fig. 9). Water molecules possibly also blocked some sites active in ammonia oxidation to N_2O and therefore increased selectivity to N_2.

The efficiency of the NH_3-SCR process is limited from the side of higher temperatures by the side reaction of direct ammonia oxidation (AMOx). The results of ammonia oxidation in the presence of Cu-Ti-FER and Cu-Ti-ITQ-6 catalysts as well as selected zeolites non-modified with copper, as reference catalysts, are shown in Fig. 12. The zeolitic samples non-modified with copper presented only very poor catalytic activity in ammonia oxidation process (Fig. 12A and B). Deposition of copper very significantly activate zeolites in the AMOx process, indicating that copper species are responsible for their activity in this reaction. Ammonia oxidation started over Cu-Ti-FER (Fig. 12A) and Cu-Ti-ITQ-6 (Fig. 12B) catalysts at about 275 and 225 °C, respectively. Assuming that the form of deposited copper determines catalytic activity of the studied samples it could be supposed that monomeric copper cations, present in the series of Cu-Ti-ITQ-6 catalysts, are more catalytically active in ammonia oxidation than aggregated copper oxide species, dominating in the Cu-Ti-FER samples (*cf.* Fig. 5B). This hypothesis is supported by the slightly higher catalytic activity of Cu-Ti-FER-25 in the AMOx process than the other samples of this series (Fig. 12A). This difference is possibly assigned to the presence of monomeric copper cations in Cu-Ti-FER-25, what was shown by UV-vis-DRS analysis (Fig. 5B). The decrease of the NO conversion due to direct ammonia oxidation in the NH_3-SCR process stared from about 300 °C (Fig. 9), while ammonia oxidation in the absence of NO started at about 225–275 °C (Fig. 12). Thus, the reduction of NO with ammonia is

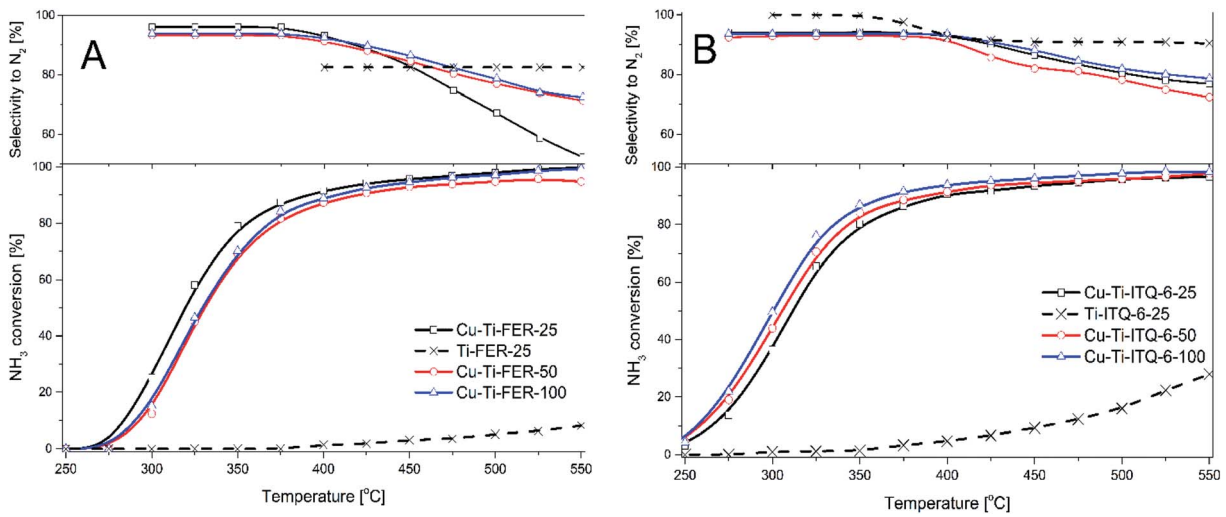

Fig. 12 Results of AMOx catalytic tests for copper modified Ti-FER (A) and Ti-ITQ-6 (B) catalysts.

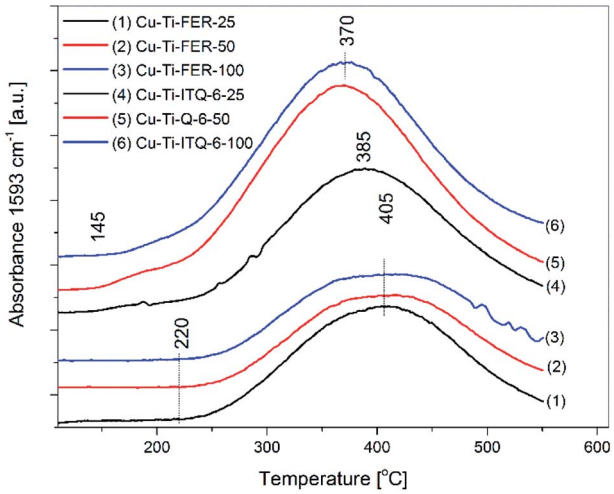

Fig. 13 Results of catalytic NO to NO_2 oxidation in the presence of copper modified Ti-FER and Ti-ITQ-6 catalysts.

preferential over direct ammonia oxidation at temperatures below 300 °C.

Low-temperature NH_3-SCR is often assigned to so called fast-SCR, which can be described by the reaction: $2NH_3 + NO + NO_2 \rightarrow 2N_2 + 3H_2O$. NO_2, which is needed for this reaction, can be formed by oxidation of NO ($2NO + O_2 \rightarrow 2NO_2$). Thus, the effective catalysts for low-temperature NH_3-SCR should be also active in the NO to NO_2 oxidation. The results of the NO to NO_2 oxidation in the presence of the studied catalysts are shown in Fig. 13. The normalized intensity of the FTIR band at 1593 cm^{-1} was used for the analysis of NO_2 formation. The NO_2 evolution started at about 220 °C and increased to about 405 °C for the series of Cu-Ti-FER catalysts. Decrease in efficiency of NO to NO_2 oxidation at higher temperatures is assigned to thermodynamical restriction of this reaction.[34] The oxidation of NO to NO_2 in the presence of Cu-Ti-ITQ-6 started at about 145 °C, so at temperature lower by 75 °C than in the case of Cu-Ti-FER catalysts. The maximum of NO_2 evolution for the Cu-Ti-ITQ-6-50 and Cu-Ti-ITQ-6-100 samples is at about 370 °C, while for Cu-Ti-ITQ-6-25 at about 385 °C. The maximal NO to NO_2 conversions, determined from the normalized intensity of 1912 cm^{-1} band (characteristic of NO), are about 20–27% for Cu-Ti-FER catalysts, 34% for Cu-Ti-ITQ-6-25 and about 48% for both Cu-Ti-ITQ-6-50 and Cu-Ti-ITQ-6-100. The catalytic activity of the studied zeolitic samples in the NO to NO_2 oxidation (Fig. 13) correlates very well with the low-temperature activity of these catalysts in NH_3-SCR (Fig. 9). Oxidation of NO to NO_2 started at lower temperatures in the presence of Cu-Ti-ITQ-6 catalysts, which presented better activity in low-temperature NH_3-SCR than Cu-Ti-FER catalysts. The Cu-ITQ-6-25 sample, that was the least active in the series of Cu-ITQ-6 catalysts, was also the least active in the NO to NO_2 oxidation in this group of the samples. Thus, it seems that the NO to NO_2 oxidation plays an important role in the activation of the low-temperature NO_x conversion over the studied catalysts. Comparison of the results of UV-vis-DRS studies (Fig. 5B) and NO to NO_2 oxidation (Fig. 13) suggests that monomeric copper cations are more catalytically active in NO oxidation than aggregated copper oxide species. Similar conclusion was reported by Shan *et al.* for Cu-SSZ-13 [35] and Liu *et al.* for ZSM-5/SAPO-34 composite catalysts.[36] Moreover, it was shown that NO_2 can be adsorbed and therefore also stabilized on the zeolite surface or may disproportionate ($2NO_2 \rightarrow NO^+ + NO_3^-$) with the formation of nitrosyl and nitrate species.[35,36] Important role of titanium in stabilization of NO_2 was also reported in literature. Raj *et al.*[21] suggested that the NO_2 molecules can be attached to the surface $\equiv$Ti–O^- groups with the formation of surface nitrates, which can easily react with ammonia. On the other hand, it was postulated by Raj *et al.*[21] and Roberge *et al.*[37] that reaction of ammonia with such surface nitrates results in reduction of Ti^{4+} cations to Ti^{3+}, which could be active sites in the NH_3-SCR reaction.

Conclusions

Copper modified titanium-ferrierites (Ti-FER) and their delaminated forms (Ti-ITQ-6) presented very promising catalytic activity in the low-temperatures NH_3-SCR process. Deposition of copper into the Ti-FER samples resulted mainly in aggregated copper oxide species, while copper in the Ti-ITQ-6 catalysts was present mainly in the form of monomeric cations. This difference in deposited copper species has been attributed to a very limited mobility of octahedral aqua copper(II) complexes in micropores of titanium ferrierites during ion-exchange process and, on the other side, no such internal diffusion limitations in the case of much larger interlayer pores in delaminated Ti-ITQ-6. Different forms of deposited copper species resulted in different properties of the catalysts in the NH_3-SCR process. Monomeric copper cations were found to be more effective in the low temperature NO conversion comparing to the more aggregated copper oxide species. The studies of the NO to NO_2 oxidation showed higher activity of monomeric copper cations in this reaction, proving that fast SCR reaction plays an important role in the low-temperature nitrogen oxides reduction with ammonia. It is postulated that dispersed copper species, active in NO to NO_2 oxidation, determines activity of the studied catalysts in the low temperature NH_3-SCR process. The selectivity to nitrogen in the NH_3-SCR process, both for the Cu-Ti-FER and Cu-Ti-ITQ-6 catalysts, was above 94% in the studied temperature range. Moreover, the Cu-Ti-ITQ-6-100 catalyst, that was found to be the most active in the standard catalytic test, presented relatively good catalytic stability in the flow of dry and wet reaction mixtures. Comparison of the Cu-Ti-ITQ-6-100 catalyst with other very active copper modified zeolites reported in scientific literature shows its great potential in the low-temperature NH_3-SCR process.

Author contributions

A. S.: methodology, investigation, data curation, writing—review & editing; A. K.: investigation; M. M.: methodology, investigation; U. D.: methodology, investigation, supervision, writing—review & editing; A. E. P.: investigation; L. C.: conceptualization, methodology, project administration, supervision, writing—original draft, writing—review & editing. All authors have read and agree to the published version of the manuscript.

Funding

This work was supported by the National Science Centre – Poland [2016/21/B/ST5/00242].

Conflicts of interest

There are no conflicts to declare.

Acknowledgements

The studies financed by National Science Centre – Poland [2016/21/B/ST5/00242]. A. Ś. has been partly supported by the EU Project POWR.03.02.00-00-I004/16. U. D. acknowledges to the Spanish Government by the funding [MAT2017-82288-C2-1-P]. Part of the research was done with equipment purchased in the frame of European Regional Development Fund (Polish Innovation Economy Operational Program [POIG.02.01.00-12-023/08]).

References

1 J. Q. Jiang, H. Pan, G. J. Sun, Z. H. Shao and Y. Shi, *Chem. Ind. Eng. Prog.*, 2012, **31**, 98.
2 R. Mrad, A. Aissat, R. Cousin, D. Courcot and S. Siffert, *Appl. Catal., A*, 2015, **504**, 542.
3 L. Han, S. Cai, M. Gao, J. Hasegawa, P. Wang, J. Zhang, L. Shi and D. Zhang, *Chem. Rev.*, 2019, **119**, 10916.
4 I. Nova, C. Ciardelli, E. Tronconi, D. Chatterjee and M. Weibel, *Top. Catal.*, 2007, **42–43**, 43.
5 G. Busca, L. Lietti, G. Ramis and F. Berti, *Appl. Catal., B*, 1998, **18**, 1.
6 D. Zhou, B. Li, Z. Ma, X. Huang, X. Zhang and H. Yang, *J. Mol. Catal. A: Chem.*, 2015, **409**, 183.
7 M. Seneque, X. Courtois, F. Can and D. Duprez, *Top. Catal.*, 2016, **59**, 938.
8 I. Nova, A. Grossaleenrico and E. Tronconi, *Chem. Today*, 2009, **27**, 17.
9 M. Mladenović, M. Paprika and A. Marinković, *Renewable Sustainable Energy Rev.*, 2018, **82**, 3350.
10 N. Akter, X. Chen, J. Parise, J. A. Boscoboinik and T. Kim, *Korean J. Chem. Eng.*, 2018, **35**, 89.
11 F. Lin, Q. Wang, J. Zhang, J. Jin, S. Lu and J. Yan, *Ind. Eng. Chem. Res.*, 2019, **58**, 22763.
12 A. Jankowska, A. Kowalczyk, M. Rutkowska, W. Mozgawa, B. Gil and L. Chmielarz, *Catal. Sci. Technol.*, 2020, **10**, 7940.
13 Y. Shan, X. Shi, J. Du, Y. Yu and H. He, *Catal. Sci. Technol.*, 2019, **9**, 106.
14 Y. Shan, X. Shi, G. He, K. Liu, Z. Yan, Y. Yu and H. He, *J. Phys. Chem. C*, 2018, **122**, 25948.
15 A. Święs, A. Kowalczyk, M. Rutkowska, U. Díaz, A. E. Palomares and L. Chmielarz, *Catalysts*, 2020, **10**, 734.
16 A. Kowalczyk, A. Święs, B. Gil, M. Rutkowska, Z. Piwowarska, A. Borcuch, M. Michalik and L. Chmielarz, *Appl. Catal., B*, 2018, **237**, 927.
17 A. C. Pradhan, B. Nanda, K. M. Parida and M. Das, *Dalton Trans.*, 2013, **42**, 558.
18 A. Jankowska, A. Chłopek, A. Kowalczyk, M. Rutkowska, W. Mozgawa, M. Michalik, S. Liu and L. Chmielarz, *Microporous Mesoporous Mater.*, 2021, **315**, 110920.
19 U. D. L. Torre, B. Pereda-Ayo and J. R. González-Velasco, *Chem. Eng. J.*, 2012, **207–208**, 10.
20 X. Feng, Q. Lin, Y. Cao, H. Zhang, Y. Li, H. Xu, C. Lin and Y. Chen, *J. Taiwan Inst. Chem. Eng.*, 2017, **80**, 805.
21 A. Raj, T. H. N. Le, S. Kaliaguine and A. Auroux, *Appl. Catal., B*, 1998, **15**, 259.
22 F. Liu, H. He, C. Zhang, Z. Feng, L. Zheng, Y. Xie and T. Hu, *Appl. Catal., B*, 2010, **96**, 408.
23 F. Liu, H. He, Y. Ding and C. Zhang, *Appl. Catal., B*, 2009, **93**, 194.
24 L. Schreyeck, P. Caullet, J. C. Mougenel, J. L. Guth and B. Marler, *Microporous Mater.*, 1996, **6**, 259.
25 R. Maddalena, C. Hall and A. Hamilton, *Thermochim. Acta*, 2019, **672**, 142.
26 M. Thommes, K. Kaneko, A. W. Neimark, J. P. Olivier, F. Rodriguez-Reinoso, J. Rouquerol and J. K. S. W. Sing, *Pure Appl. Chem.*, 2015, **87**, 1051.
27 M. Thommes, *Chem. Ing. Tech.*, 2010, **82**, 1059.
28 H. Hu, M. Ke, K. Zhang, Q. Liu, P. Yu, Y. Liu, C. Li and W. Liu, *RSC Adv.*, 2017, **7**, 31535.
29 M. Radko, M. Rutkowska, A. Kowalczyk, P. Mikrut, A. Święs, U. Díaz, A. E. Palomares, W. Macyk and L. Chmielarz, *Microporous Mesoporous Mater.*, 2020, **302**, 110219.
30 A. Corma, U. Díaz, M. E. Domine and V. Fornés, *J. Am. Chem. Soc.*, 2000, **122**, 2804.
31 X. Yang, X. Wang, X. Qiao, Y. Jin and B. Fan, *Materials*, 2020, **13**, 888.
32 J. A. Sullivan and J. Cunningham, *Appl. Catal., B*, 1998, **15**, 275.
33 C. Borgida, F. Boscherini, S. Caluccia, F. Genoni, C. Lamberti, L. Marchese, G. Petrini, C. Vlaich and A. Zecchina, *Catal. Lett.*, 1994, **26**, 195.
34 G. Qi and W. Li, *Catal. Today*, 2015, **258**, 205.
35 Y. Shan, Y. Sun, J. Du, Y. Zhang, X. Shi, Y. Yu, W. Shan and H. He, *Appl. Catal., B*, 2020, **32**, 119105.
36 J. Liu, W. Song, C. Xu, J. Liu, Z. Zhao, Y. Wei, A. Duan and G. Jiang, *RSC Adv.*, 2015, **5**, 104923.
37 D. Roberge, A. Raj, S. Kaliaguine, D. T. On, S. Iwamoto and T. Inui, *Appl. Catal., B*, 1996, **10**, L237.